# Suppression of Inflammation Delays Hair Cell Regeneration and Functional Recovery Following Lateral Line Damage in Zebrafish Larvae

Ru Zhang[1,2,3], Xiao-Peng Liu[3,4], Ya-Juan Li[2], Ming Wang[1,3], Lin Chen[1,3*], Bing Hu[1,2*]

1 CAS Key Laboratory of Brain Function and Diseases, School of Life Sciences, University of Science and Technology of China, Hefei 230027, China.

2 Lab of Neurodevelopment and Repair, University of Science and Technology of China, Hefei 230027, China.

3 Auditory Research Laboratory, University of Science and Technology of China, Hefei 230027, China.

4 Center for Hearing and Deafness, State University of New York at Buffalo, NY14214, USA.

**[*]Corresponding authors.**

Bing Hu, PhD, Lab of Neurodevelopment and Repair, University of Science and Technology of China, Hefei 230027, China.

Tel.: +86 (551) 6360-2489

E-mail: bhu@ustc.edu.cn

Lin Chen, PhD, Auditory Research Laboratory, University of Science and Technology of China, Hefei 230027, China.

Tel.: +86 (551) 6360-7623

E-mail: linchen@ustc.edu.cn

## Abstract:

**Background:** Human cochlear hair cells cannot spontaneously regenerate after loss. In contrast, those in fish and amphibians have a remarkable ability to regenerate after damaged. Previous studies focus on signaling mechanisms of hair cell regeneration, such as Wnt and Notch signals but seldom on the fact that the beginning of regeneration is accompanied by a large number of inflammatory responses. The detailed role of this inflammation in hair cell regeneration is still unknown. In addition, there is no appropriate behavioral method to quantitatively evaluate the functional recovery of lateral line hair cells after regeneration.

**Results:** In this study, we found that when inflammation was suppressed, the regeneration of lateral line hair cells and the recovery of the rheotaxis of the larvae were significantly delayed. Calcium imaging showed that the function of the neuromasts in the inflammation-inhibited group was weaker than that in the non-inflammation-inhibited group at the Early Stage of regeneration, and returned to normal at the Late Stage. Calcium imaging also revealed the cause of the mismatch between the function and quantity during regeneration.

**Conclusions:** Our results, meanwhile, suggest that suppressing inflammation delays hair cell regeneration and functional recovery when hair cells are damaged. This study may provide a new knowledge for how to promote hair cell regeneration and functional recovery in adult mammals.



**Keywords:** inflammation, hair cell regeneration, neuromast, lateral line, zebrafish larva, rheotaxis, calcium imaging.

## Background:

Deafness and hearing defects are usually caused by loss of sensory hair cells or defect of auditory function. The loss of hair cells is result of aging, infection, genetic factors, hypoxia, autoimmune disorder, ototoxic drugs or noise exposure. Unfortunately, including humans, hair cells cannot regenerate in mammals (Oesterle and Stone, 2008; Yorgason. et al., 2006). In contrast, hair cells in some non-mammalian vertebrates have a remarkable ability to regenerate, such as birds, reptiles, amphibians and fish (Matsui. and Cotanchea., 2004; Popper and Hoxter, 1984; Stone. and Rubel., 2000). It could suggest that if we figure out the mechanism of hair cell regeneration in these species, we probably can promote hair cell regeneration in mammals.

When hair cells are damaged, support cells proliferate into both hair cells and support cells, or convert into hair cells directly (Baird et al., 1996; Lopez-Schier and Hudspeth, 2006; Raphael, 1992; Roberson et al., 2004). Hair cell regeneration is finely regulated by the interaction of multiple signaling pathways, such as Notch signaling (Ma et al., 2008; Mizutari et al., 2013), Wnt/b-catenin signaling (Aman and Piotrowski, 2008; Chai et al., 2012; Shimizu et al., 2012), Fgf signaling (Aman and Piotrowski, 2008; Nechiporuk and Raible, 2008), retinoic acid (Rubbini et al., 2015) and so on. In the process of hair cell damaged, it is accompanied by a lot of inflammatory reaction, which has been found to play a role in tissue regeneration in recent years (Mescher, 2017). For example, macrophages are considered having main function in the inflammatory resolution stage and being required for fin regeneration (Li et al., 2012) and hair cell regeneration in zebrafish (Carrillo et al., 2016). In addition, it has been confirmed that neutrophils in mice play a central role in inflammation-induced optic nerve regeneration (Kurimoto et al., 2013).

In recent years, zebrafish (Danio rerio) has become an ideal model for studying inflammation and hair cell regeneration because it has conservative

84 innate immunity (Renshaw and Trede, 2012) and strong regeneration ability in
85 lateral line system (Lush and Piotrowski, 2014) which makes zebrafish larvae
86 to perceive the change of surrounding flow, detect their prey and avoid
87 predators (Coombs. et al., 2014; Dijkgraaf, 1962). The lateral system of a larva
88 is composed of neuromasts which located on the surface of the body.
89 The neuromasts on the head consist of the anterior lateral line system (aLL)
90 and the ones along the body comprise the posterior lateral line system
91 (pLL)(Thomas et al., 2015). The center of the neuromast is composed of hair
92 cells and they are surrounded by support cells and mantle cells. At the top of
93 the hair cells, rows of short stereocilia and a long kinocilium extend out of the
94 body called the hair bundle and are covered in a gelatinous cupula. The
95 arrangement of stereocilia and kinocilium determines the polarity of hair cells
96 and the polarity of the hair cells is planar cell polarity (PCP), which is arranged
97 symmetrically (Flock and Wersall, 1962), half in each direction.

98 When hair bundles are deflected, hair cells release transmitters and cause
99 exciting spikes in afferent neurons (Dijkgraaf, 1962). And then, larvae show a
100 robust behavior called rheotaxis (Olszewski et al., 2012). This behavior can be
101 applied to evaluate the function of hair cells (Suli et al., 2012).

102 In recent years, calcium imaging has become a popular method to
103 measure the function of neural cells in detail and quantitatively (Zhang et al.,
104 2016). When the mechanical hair bundle deflected, calcium and other cations
105 enter into cytoplasm through mechanotransduction channels. It changes the
106 membrane potential and activates voltage-gated calcium channels which allow
107 rapid calcium inflow to trigger synaptic transmission. GCaMPs, a
108 genetically-encoded calcium indicator(GECIs), are single fluorescent proteins,
109 which can bind calcium directly and alter conformation to respond the change
110 of calcium concentration (Tian et al., 2012). These significant,
111 activity-dependent signals can reflect the function of hair cells in a single

112 neuromast (Zhang et al., 2018; Zhang et al., 2016).

113 Previous research has found that the deletion of macrophages by
114 morpholino leads to the delay of hair cell regeneration (Carrillo et al., 2016).
115 However, does it still cause the delay of hair cell regeneration when the
116 macrophages are intact, and the pro-inflammatory factors are suppressed as
117 the hair cells are damaged? Is there any delay in the functional recovery of the
118 lateral line?

119 In order to figure out the above problems, we used an anti-inflammatory
120 agent, BRS-28, to suppress the inflammation when hair cells are damaged by
121 copper. BRS-28 is a derivative of 5α-cholestan-6-one, which was confirmed to
122 be a remarkably suppressor of the production of pro-inflammatory factors,
123 such as NO, TNF-α、IL-1β、iNOS and cox-2 (Yang et al., 2014). We count the
124 number of neutrophils and macrophages in Tg(corola-eGFP; lyz-Dsred)
125 transgenic line. Then, AB/WT zebrafish larvae were used to count the number
126 of regenerated hair cells. Since there is no appropriate behavioral method to
127 quantitatively evaluate the function of lateral line hair cells, we designed and
128 built devices to test rheotaxis behavior in AB/WT larvae. A behavioral analysis
129 software was applied for quantitative evaluation of rheotaxis, so as to reflect
130 the holistic functional recovery of the posterior lateral line. Finally, the function
131 of the regenerated hair cells in a single neuromast was evaluated by the
132 method of calcium imaging in Huc:h2b-gcamp6f transgenic line.

133

# 134 Results

### 135 $CuSO_4$ damaged hair cells in lateral line of zebrafish.

136 Sensory hair cells in a 6-day post fertilization (dpf) AB/WT zebrafish larva
137 were labeled with 0.05% DASPEI clearly (**Fig. 1A**). L2、LII3、L3 neuromasts
138 (circles in **Fig.1 A**) were three of the posterior lateral neuromasts, which

139 located along the flat truck body and easily to be observed. A lateral view of the
140 neuromasts showed the elongated kinocilia extending from the body (**Fig. 1B**).
141 The neuromasts are consisted of hair cells surrounded by support cells, which
142 are surrounded by mantle cells (**Fig. 1C**). In order to study the effects of
143 inflammation on hair cell regeneration, we established a hair-cell-damaged
144 model. Hair cells were damaged completely, when treated with 5 μM $CuSO_4$
145 for 1 h (**Fig. 1D**). Labeled with 0.05% DASPEI, hair cells displayed close
146 arrangement and clear boundary. Only treated with $CuSO_4$ solution for 20 min,
147 hair cells became loose and unclear which suggested that they were already
148 injured. The number of hair cells decreased with weaker fluorescence intensity
149 and obscure cell boundary at 40 min. Hair cells were completely disappeared
150 at 60 min, indicating that they had been completely damaged. TUNEL assay
151 revealed the missing hair cells underwent apoptosis (**Supplementary Fig. 1**).
152 After being transferred to embryo medium (EM), the number of hair cells
153 quickly returned to normal (**Fig. 1E**).

154 **BRS-28 reduced the number of neutrophils and macrophages migrating**
155 **to the injured neuromasts.**

156 Neutrophils (**Fig. 2B, C**, blue arrows) and macrophages (**Fig. 2B, C**, white
157 arrows) could be marked and distinguished in larvae of Tg(corola-eGFP;
158 lyz-Dsred) transgenic line (**Supplementary Fig. 2**). Normally, neutrophils and
159 macrophages were almost absent from the neuromasts (example, **Fig. 2A**).
160 When treated with $CuSO_4$ solution, hair cells were damaged. Neutrophils and
161 macrophages migrated to the neuromasts within 1 hours (example, **Fig. 2B**).
162 When larvae were immerged in BRS-28, an anti-inflammatory agent, before
163 treated with $CuSO_4$ solution, less neutrophils and macrophages migrated to
164 the damaged neuromasts (example, **Fig. 2C**). When the inflammation
165 suppressed, the numbers of neutrophils appeared around the damaged
166 neuromasts were lower at 0.5,1,3 and 4 h after adding the $CuSO_4$ solution in

167 BRS+$CuSO_4$ group than in $CuSO_4$ group (**Fig. 2D**). In addition, we observed
168 BRS+$CuSO_4$ group had fewer macrophages at 0.5, 1, 2 and 3 h than $CuSO_4$
169 group (**Fig. 2E**). Collectively, the data strongly suggested that BRS-28 reduced
170 the number of neutrophils and macrophages migrating to the injured
171 neuromasts. It was worth noting that compared with control, there was no
172 significant difference in the numbers of neutrophils and macrophages between
173 $CuSO_4$ group and BRS+$CuSO_4$ group at 5 and 6 h, indicating that the
174 inflammation was almost resolved.

175 **Suppressing inflammation delayed hair cell regeneration.**

176 In order to investigate whether the regeneration of hair cells were delayed
177 after suppressing inflammation, we observed hair cells in the L2, LII3 and L3
178 neuromasts. We found that the regeneration of hair cells was delayed after the
179 inflammation was suppressed by the inflammatory inhibitor, BRS-28. Live
180 imaging showed regenerated hair cells in $CuSO_4$, BRS+$CuSO_4$ group at 24, 48
181 and 96 hours post injured (hpi) by $CuSO_4$(**Fig. 3A**). Control group was showed
182 at the same time point. Further analysis revealed that the numbers of
183 regenerated hair cells were significantly decreased in BRS+$CuSO_4$ group than
184 that in $CuSO_4$ group at 16 hpi ($P=0.0061$), 24 hpi ($P=0.0021$) and 48 hpi
185 ($P<0.0001$) (**Fig. 3B**, n = 30 neuromasts). These results indicated that the
186 regeneration of hair cells was delayed in BRS+$CuSO_4$ group within 48 hpi.
187 Compared with Control group, there was no difference in the number of hair
188 cells between $CuSO_4$ group and BRS+$CuSO_4$ group at 96 hpi, suggesting that
189 hair cells were regenerated to the normal level at 96 hpi. We also analyzed the
190 number of hair cells when only treated with BRS-28 (BRS group) without hair
191 cell damage. As expected, BRS group had no difference compared with
192 Control group at any time point, excluding the effect of BRS-28 on hair cells.

193 Since hair cells did not regenerate at a uniform rate, we defined the time
194 of regeneration into two periods: the Early Stage which includes the time from

195 0 to 48 hpi and the Late Stage which includes the time after 48 hpi. The
196 regeneration of hair cells was fast in the Early Stage and slow in the Late
197 Stage. Linear analysis was conducted on the number of hair cell regeneration
198 in the Early Stage. The slope in $CuSO_4$ group (0.1879) was higher than that in
199 BRS+$CuSO_4$ group (0.148) , meanwhile, x-intercept in $CuSO_4$ group (4.16)
200 was higher than that in BRS+$CuSO_4$ group (8.287) (**Fig. 3C, D**). These implied
201 that the hair cell regeneration in BRS+$CuSO_4$ group may begin later and
202 slower than that in $CuSO_4$ group.

203 To explore whether the time window of inflammatory suppression had
204 contribute to delayed regeneration, we changed the start time of BRS-28
205 treatment. We found that compared with the $CuSO_4$ group, whether BRS-28
206 was added at the same time as $CuSO_4$ ($CuSO_4$+BRS 0 h group), or 30 minutes
207 after the addition of $CuSO_4$ ($CuSO_4$+BRS 0.5 h group), or 1 hour after the
208 addition of $CuSO_4$ ($CuSO_4$+BRS 1 h group) (**Fig. 3E**), there was no statistical
209 difference on the number of regenerated hair cells.

210 To sum up, the regeneration of hair cells in lateral line was delayed after
211 the inflammation was suppressed by the inflammatory inhibitor BRS-28.

212 **The functional recovery of the lateral line system was delayed when**
213 **inflammation was suppressed.**

214 Since the rheotaxis could be a suitable functional readout of the lateral
215 line, we designed a behavioral device to test the rheotaxis of zebrafish (**Fig.**
216 **4A**, see details in Materials and Methods). Larvae were placed from the right
217 platform, and they sense the water flow direction from the right to the left.
218 **Figure 4B, C** were two examples of the larval rheotaxis processed by
219 behavioral analysis software: the former was a larva with excellent rheotaxis
220 (**Fig. 4B**) while the latter was a larva performed failure in the rheotaxis test (**Fig.**
221 **4C**). The left panels in these two examples showed the swimming track of this
222 larva. The behavioral analysis software mapped its movement path of larvae

223 by line segment. The color of the line segment represented the direction of
224 movement of the larvae. All the movements from right to left were represented
225 by purplish or red segments, where purple indicated that the velocity along the
226 flow direction was greater than or equal to the flow velocity, and red indicated
227 that the velocity along the flow direction was less than the flow velocity. All the
228 movements from left to right were represented by green segments, and the
229 higher the brightness was, the faster the speed was. The right panels
230 displayed the motion vector. The lengths of the blue segments represented the
231 distance of each movement, and the direction of the blue segment represented
232 the direction of that movement. The length of the red line segment was the
233 ratio of motion vectors sum to the motion arithmetic sum and the direction was
234 the direction of the sum of the vectors.

235 When the red segment was long and had a small angle of 0 degree, it
236 indicated that the motion of the larva was consistent with the opposite direction
237 of flow. It represented that the larva had a good rheotaxis, indicating its lateral
238 line system executed its function very well. Therefore, the software reported a
239 high score. On the contrary, when the red segment was short or had a small
240 angle of 180 degree, it indicated that the larva moved randomly and had a poor
241 rheotaxis, indicating its lateral line system had poor function. In this case, the
242 software reported a low score. The scores reported by the software were
243 plotted into bar charts and showed in **Figure 4D**. After the hair cells were
244 damaged by $CuSO_4$, there was poor rheotaxis in both $CuSO_4$ group and
245 BRS+$CuSO_4$ group. At 24 and 48 hpi, the rheotaxis of BRS+$CuSO_4$ group was
246 significantly lower than that of Control group. On the contrary, the rheotaxis of
247 $CuSO_4$ group was not significantly different from that of Control group within 24
248 hpi. Therefore, it indicated that the functional recovery of lateral line system
249 was delayed in BRS+$CuSO_4$ group. The rheotaxis of BRS group at each time
250 point was not different from that of Control group, suggesting that BRS-28

251 alone had no significant effect on the rheotaxis. In addition, we noted that the
252 speed and distance of each movements were consistent within different times
253 and between different groups: both were stable at around 22 mm/s (**Fig. 4E, F**),
254 which indicated that BRS-28 or $CuSO_4$ did not affect the movement of
255 zebrafish.

256 We concluded that the regenerated hair cells still had the ability to sense
257 water flow, but the functional recovery of lateral line system was delayed when
258 inflammation was suppressed.

259 **Calcium imaging revealed the function of a single neuromast after hair**
260 **cell regeneration**

261 Since we found a mismatch between the function of the lateral line and the
262 amount of hair cell regeneration, that is, after the zebrafish lateral line was
263 damaged by copper sulfate, it took 96 h for the hair cells to return to normal,
264 while the flow ability returned to normal at 24 h. The function of a single
265 neuromast can be evaluated by observing its calcium activity (Zhang et al.,
266 2016). The L3 neuromast, located in flat trunk, was stimulated by water flow
267 from an electrode (**Fig. 5A**). Since hair cells had polarities, the yellow and
268 green hair cells represented opposite polarities. Chou et al. reported that the
269 polarity of the L3 neuromast is parallel to the anterior-posterior body axis
270 (Chou et al., 2017). Thus, by adjusting the direction of the electrode, water was
271 controlled to flow in two directions: anterior to posterior (A-P) direction or
272 posterior to anterior (P-A) direction. We found that not all hair cells responded
273 to the water flow, and only some hair cells were active (example, **Fig. 5B**,
274 circled cells). These active cells only responded to stimulus in one direction:
275 P-A direction (**Fig. 5C**, yellow ones and yellow circles in **Fig. 5B**) or A–P
276 direction (**Fig. 5D**, green ones and green circles in **Fig. 5B**). Because the
277 neuromasts were stereoscopic, some of the active hair cells were far from this
278 focal plane (dashed circles in **Fig. 5B**) and were not included in subsequent

279 fluorescence intensity analysis.

280 Similar to the results of the rheotaxis, the fluorescence intensity (ΔF/F) of
281 the regenerated hair cells were reduced significantly when inflammation was
282 suppressed at the Early Stage of regeneration (within 48 hpi)(**Fig. 5E**). It was
283 noteworthy that compared to Control group, the fluorescence intensity in
284 $CuSO_4$ group did not decrease significantly in the Early Stage of regeneration.
285 This might explain that why the rheotaxis in $CuSO_4$ group had been recovered
286 at 24 hpi. The fluorescence intensity of BRS+$CuSO_4$ group was not
287 significantly different from that of Control group and $CuSO_4$ group in the Late
288 Stage of regeneration (72-96 hpi) (**Fig. 5F**). Additionally, the fluorescence
289 intensity showed no differences between the BRS group and Control group
290 (**Fig. 5G**), indicating that BRS-28 had no effect on the fluorescence intensity.

291 Normally, only a part of the hair cells in the neuromast responds to the
292 stimulation of water flow. Is it the same for regenerated hair cells? We found
293 that only a few regenerated hair cells in $CuSO_4$ group and BRS+$CuSO_4$ group
294 responded to flow stimuli. The number of active cells in each neuromast in
295 these two group were approximately the same at 24 to 96 hpi, and were
296 consistent with that in Control group (**Fig. 5H**).

297 Furthermore, we noticed that most hair cells that responded to the flow in
298 the opposite direction came in pairs (**Supplementary Fig. 3A**). Although the
299 numbers of hair cells responding to flow in P-A direction were similar to that in
300 A-P direction, the fluorescence intensity of hair cells responding to P-A
301 direction was significantly higher than that of hair cells responding to A-P
302 direction (**Supplementary Fig. 3B**). It indicated that L3 neuromast was more
303 sensitive to the flow from the P-A direction.

304 The results altogether demonstrated that the recovery of hair cell function
305 was delayed at the Early Stage of regeneration when inflammation was
306 suppressed.

307

308 # Discussion

309 **BRS-28 suppresses inflammation and delays the initiation of hair cell**
310 **regeneration.**

311 Although the downregulation of Notch signal during lateral line
312 regeneration induces the proliferation of support cells by activating
313 Wnt/b-Catenin signal (Romero-Carvajal et al., 2015), it is still unknown how the
314 downregulation of Notch signal is triggered after hair cell death. Kniss et al.
315 propos a hypothesis of triggering hair cell regeneration (Kniss et al., 2016).
316 Studies in Drosophila wing disc and eye have found that JNK, Shh, EGF, and
317 TNF signaling pathways are required during apoptosis-induced compensatory
318 proliferation (Fan et al., 2014; Perez-Garijo et al., 2009; Ryoo et al., 2004).
319 Kniss et al. assume that a similar process may be involved in the regeneration
320 of hair cells. On the basis of this hypothesis, we speculate that when hair cells
321 are damaged by $CuSO_4$, it cause apoptosis in lateral line hair cells, trigger the
322 rise of reactive oxygen species (ROS) and reactive nitrogen species (RNS),
323 and induce the oxidative stress. This process may improve AP-1,HIF-1α and
324 NF-κB activity, and thus increase pro-inflammatory cytokines and chemokines,
325 such as NO, IL-1β, TNF-α, cox-2,iNOS and so on (Pereira et al., 2016).
326 BRS-28, suppress the production of NO、IL-1β、TNF-α、cox-2、iNOS (Yang et
327 al., 2014), reducing the number of neutrophils and macrophages migrating to
328 the damage of neuromasts. Besides that, the decrease of pro-inflammatory
329 factors may reduce the activation of macrophages. These processes would
330 decrease the production of TNF ligands and inhibit the JNK signal, which
331 contributes to initiating cells regeneration, and eventually leads to delay
332 initiation of compensatory proliferation and delay regeneration of hair cells.

333 We found that when the initiate time of inflammatory inhibitors was
334 changed, there was no delay in hair cell regeneration (**Fig. 3E**). This also

335 suggests that the timing of inflammation suppression is important: when
336 inflammation occurs, compensatory proliferation of the support cells is
337 triggered and hair cells begin to regenerate. If inflammation suppression does
338 not take effect, regeneration seems to be unaffected.

339 In addition, neutrophils can also remove dead cell debris, and
340 macrophages can phagocyte apoptotic neutrophils or fragments of dead cells.
341 We believe that when the number and activity of neutrophils and macrophages
342 decrease, the clearance of damaged tissue areas slows down, and hair cells
343 cannot obtain a good regeneration environment. Since damaged neuromasts
344 need more time to clean up these cell fragments, this may also delay the
345 regeneration of hair cells.

346 **Suppression of inflammation delays functional recovery of regenerated**
347 **hair cells.**

348 In this study, we found that when inflammation was suppressed, hair cell
349 regeneration was delayed, as was the recovery of function. Finally, the quantity
350 and the function of hair cells returned to normal level at the Late Stage of
351 regeneration. Therefore, although the suppression of inflammation delayed the
352 regeneration of hair cells, it did not affect the overall process of hair cell
353 regeneration, and the function of regenerated hair cells eventually tended to be
354 intact. However, the effect of inflammation on the regeneration of lateral hair
355 cells seems to be different from that of the fin. Li et al. found that when
356 zebrafish larvae lack macrophages, vacuoles appear in the regenerated fin,
357 suggesting that macrophages may also be involved in fin regeneration (Li et al.,
358 2012). In our research, although the suppression of inflammation delay
359 regeneration of hair cells and their functional recovery at the Early Stage of
360 regeneration, they eventually return to the normal status at the Late Stage of
361 regeneration. This is not because inflammation is not suppressed sufficiently,
362 as Carrillo et al. found that the number of hair cells finally completed

363 regeneration even when macrophages is knockout (Carrillo et al., 2016).
364 However, this may be because the injured organs are different, and the intact
365 function of lateral hair cells is crucial for the survival of zebrafish. It is
366 suggested that the hair cells in lateral line may have more complex regulation
367 mechanisms during the regeneration process.

368 **The functional recovery of hair cells is much faster than its quantity.**

369 Previous studies have focused on the morphological and quantitative
370 recovery of regenerated hair cells in zebrafish (Carrillo et al., 2016;
371 Romero-Carvajal et al., 2015). Since the regeneration takes 3-4 days post
372 injured, it is easy to assume that the recovery of the function of the neuromasts
373 may be proportional to the number of regenerated hair cells. In this study, for
374 the first time, we performed a method to evaluate the function of regenerated
375 hair cells. We found that the $CuSO_4$ group already performed excellent
376 rheotaxis at 24 hpi (**Fig. 4C**), even though the average number of hair cells
377 was only 3.667 at that time (**Fig. 3B**). Therefore, hair cells recover the function
378 much more quickly than their numbers. In other words, although it takes 72-96
379 h to complete regeneration, the function of hair cells can be recovered within
380 24 hours which is critical for the survival of zebrafish. When BRS-28 is used to
381 suppress the inflammation, the amplitude of calcium activity of hair cells is
382 significantly lower than that of Control and $CuSO_4$ group at the Early Stage of
383 regeneration, and the rheotaxis of larvae is poor during this period. Therefore,
384 the suppression of inflammation not only delays the hair cell regeneration, but
385 also delays the functional recovery.

386 There is a mismatch between the function and quantity during
387 regeneration. Calcium image reveal that only a part of regenerated hair cells in
388 one neuromast respond to the flow. This finding is consistent with previous
389 study (Zhang et al., 2018). In our research, we found that this phenomenon
390 also exists in regeneration group ($CuSO_4$ and BRS+$CuSO_4$ group).

391 Regardless of the number of regenerated hair cells, the number of hair cells
392 that respond to water flow remain stable during the regeneration process,
393 which is not different from Control group (**Fig. 5H**). Besides that, in the Early
394 Stage of regeneration, the magnitude of fluorescence intensity and reaction
395 time of $CuSO_4$ group are also consistent with that of the controls. This explains
396 why the number of regeneration in the $CuSO_4$ group at 24 h is only 3.667 on
397 average, but the function of the lateral line has been restored to a level very
398 close to that of Control group.

399 In this study, we only performed calcium imaging on the L3 neuromast,
400 which was confirmed as the polarity of the A-P body axis in the study of Chou
401 et al (Chou et al., 2017). Consistent with their results, this neuromast is indeed
402 insensitive to the flow in the dorsal-ventral (D-V) body axis (data not shown).
403 Therefore, this study only focuses on the stimulus response in the A-P body
404 axis direction, and does not further analyze the stimulus data in the D-V body
405 axis direction. Compared with hair cells with polarity in the A-P direction, hair
406 cells with polarity in the P-A direction have greater ΔF/F0 when stimulated by
407 water flow (**Supplementary Fig. 3B**; sample, **Fig. 5 C, D**). It indicated that L3
408 neuromast is more sensitive to the flow from the P-A direction. This finding is
409 consistent with the results measured by Chou et al. using microphonic
410 potentials evoked by sinusoidal stimuli (Chou et al., 2017). Most active hair
411 cells that responded to the opposite flow come in pairs (**Supplementary Fig.
412 3A**), suggesting that it appears to be pre-arranged rather than random.

413 In summary, our research suggests that suppression of inflammation
414 delays functional regeneration of lateral hair cells in zebrafish larvae. The
415 inflammation plays positive and permissive roles in hair cell regeneration.

416

417 # Materials and Methods

418 **Zebrafish strains and maintenance**

419 AB/Wild-type strain, Tg(corola-eGFP;lyz-Dsred) and Huc:h2b-gcamp6f
420 transgenic line were used in this study. Embryos were generated by paired
421 mating and maintained at 28.5℃ in EM and on a 14/10 h light/dark cycle
422 according to the standard protocols.
423 All animal manipulations were conducted strictly in accordance with the
424 guidelines and regulations set forth by the University of Science and
425 Technology of China (USTC) Animal Resources Center and the University
426 Animal Care and Use Committee. The protocol was approved by the
427 Committee on the Ethics of Animal Experiments of the USTC (Permit Number:
428 USTCACUC1103013).
429 **Hair cell damage and inflammation inhibition**
430 In order to damage hair cells in lateral line, 4 dpf Larvae were treated with
431 5 μM $CuSO_4$ (Sangon, China) diluted in embro medium (EM) for 1 h. Then,
432 they were washed three times and recovered in EM.
433 To suppress inflammation, 4 dpf larvae were immersed in 0.1% BRS-28,
434 an anti-inflammatory agent, for 3 h before being moved into $CuSO_4$ to damage
435 hair cells.
436 **Live imaging**
437 AB/Wild-type larvae were used to count the number of regenerated hair
438 cells in L2、LII3、L3 neuromasts (**Fig. 1A**). Hair cells were marked by
439 0.01 %DAPI for 5 minutes. Larvae were anesthetized in 0.02% MS-222
440 (Tricaine mesylate, Sigma, USA) and imaged under a fluorescence
441 microscope (Olympus BX-60, Japan).
442 In order to exhibit the damage of hair cells in copper sulfate solution and
443 the regeneration of hair cells in different phases, hair cells were labeled by
444 0.05 % DASPEI (Sigma, USA), and larvae were anesthetized in MS-222 and
445 imaged under a confocal microscopy (Zeiss LSM 880 +Airyscan, Germany).
446 Tg(corola-eGFP; lyz-Dsred) transgenic line was used to observe the

447 number of neutrophils and macrophages migrating to the injured neuromasts
448 *in vivo*. In this transgenic line, neutrophils co-expressed *lyz-Dsred* and
449 *coro1a-GFP* and show yellow fluorescence after these two channels are
450 merged, while macrophages only express *coro1a-GFP* and show green
451 fluorescence (Li et al., 2012). To show the neutrophils and macrophages
452 migrating to damaged neuromasts, larvae were anesthetized in MS-222 and
453 imaged under a confocal microscopy (Zeiss LSM 880 +Airyscan). In order to
454 count neutrophils and macrophages, we set the area around the L2 LII3 L3
455 neuromasts with a diameter of 100 μm as the region of interest (ROI).
456 Zebrafish larvae were anesthetized and imaged by the fluorescence
457 microscope (Olympus BX-60) with a green and a red channel.

458 **Rheotaxis behavior experiments**

459 A U-shaped tank was designed to test the rheotaxis behavior of larvae
460 (**Fig. 4A**). The bottom of the two cubic tanks (7 cm length *8 cm width*8 cm
461 height) were connected by a platform (10 cm length *8 cm width*0.5 cm height).
462 A peristaltic pump (Longer Pump YZ1515x, China) was used to move EM
463 solution from the left tank to the right tank, so that the platform formed a steady
464 water flow from right to left (v=10 mm/s). AB/WT zebrafish larvae were applied
465 to detect the ability of rheotaxis. Larvae were released at the right side of the
466 platform with an initial velocity almost equals 0. To avoid visual cues,
467 experiments were operated in the dark and rheotaxis performs were recorded
468 by an infrared CCD (IR850, weixinshijie, China).

469 Rheotaxis data were analyzed by our own rheotaxis software edited in
470 Matlab (2015a, MathWorks, USA). This software can plot the movement track
471 of zebrafish larvae in the platform, measure the direction and distance of each
472 swimming and calculate the speed. Finally, it reports scores based on the
473 magnitude in the horizontal direction of the ratio of motion vectors sum to the
474 motion arithmetic sum.

475 **Calcium imaging and data analyses**

476 Huc: h2b-GCamp6f transgenic line was used in calcium imaging which
477 expressed pan-neuronal nucleus-labelled GCamp6f. Larvae were
478 anesthetized and fixed by a net pressure. The one-step pulled micropipette
479 had a long, wispy tip which must be trimmed by rubbing it against with another
480 pulled micropipette to generate a tip with an outer diameter of approximately
481 40 μm. The micropipette was filled with 0.02% MS-222 and fixed to the holder
482 of a micromanipulator (MX7500, Scientific Design Company, USA). The tip of
483 the micropipette was positioned at a distance of approximately 100 μm from
484 the top of the kinocilia (**Fig. 5A**). The duration of flow was controlled by
485 three direct links which were linked with a syringe.

486 Calcium imaging was collected by a confocal microscopy (FV 1000,
487 Olympus, Japan). To make as many hair cells as possible in the observation
488 area at the same time, a single z-axis was adjusted. ROI was set to 110*108.
489 We took 100 time-lapse images for each neuromast, and the total capture time
490 was 29.7 s (0.297 s per slice). Flow stimulation occurred from 10.098 to 19.899
491 s.

492 Since the neuromasts are three-dimensional, different hair cells have
493 different levels of fluorescence intensity. Namely, they have different levels of F
494 prime. The relative fluorescence intensity change ($\Delta F/F_0$) is more commonly
495 used. For each hair cell, the average fluorescence intensity before flow stimuli
496 (0-10 s) was set as $F_0$. The data would be excluded when $F_0<95$, which means
497 these hair cells were too far from the focal plane. When more than two hair
498 cells in the neuromast respond to flow stimulation, two hair cells with the
499 strongest fluorescence were selected and included in the statistics of
500 fluorescence intensity curve.

501 **Statistical analysis**

502 All data were shown as mean ± S.E.M. or as relative proportions of 100 %

503 as indicated in the appropriate legends. The data were analyzed in either
504 one-way ANOVA with Tukey's multiple comparisons test or two-way ANOVA
505 with Tukey's multiple comparisons test by GraphPad Prism version 7.0 (Prism,
506 San Diego, CA, USA). The level of significance was set to $P < 0.05$. *, **and
507 ***represent $P < 0.05$, $P < 0.01$ and $P < 0.001$, respectively.
508

509 # Acknowledgments

510 The authors thank Drs. Wen Zilong for providing the Tg(corola-eGFP;
511 lyz-Dsred) transgenic fish line, Drs. Wen Quan for providing the
512 Huc:h2b-gcamp6f transgenic fish line. The authors thank Drs. Zhen Xuechu for
513 providing BRS-28 and the compound-26 in their study is the BRS-28
514 mentioned in this study.

515

516 # References

517 **Aman, A., and Piotrowski, T. (2008). Wnt/beta-catenin and Fgf signaling control collective**
518 **cell migration by restricting chemokine receptor expression. Developmental cell *15*, 749-761.**
519 **Baird, R.A., Steyger, P.S., and Schuff, N.R. (1996). Mitotic and nonmitotic hair cell regeneration**
520 **in the bullfrog vestibular otolith organs. Annals of the New York Academy of Sciences *781*, 59-70.**
521 **Carrillo, S.A., Anguita-Salinas, C., Pena, O.A., Morales, R.A., Munoz-Sanchez, S.,**
522 **Munoz-Montecinos, C., Paredes-Zuniga, S., Tapia, K., and Allende, M.L. (2016). Macrophage**
523 **Recruitment Contributes to Regeneration of Mechanosensory Hair Cells in the Zebrafish Lateral Line.**
524 **Journal of cellular biochemistry *117*, 1880-1889.**
525 **Chai, R., Kuo, B., Wang, T., Liaw, E.J., Xia, A., Jan, T.A., Liu, Z., Taketo, M.M., Oghalai, J.S., Nusse,**
526 **R.*, et al.* (2012). Wnt signaling induces proliferation of sensory precursors in the postnatal mouse**
527 **cochlea. Proceedings of the National Academy of Sciences of the United States of America *109*,**
528 **8167-8172.**
529 **Chou, S.W., Chen, Z., Zhu, S., Davis, R.W., Hu, J., Liu, L., Fernando, C.A., Kindig, K., Brown, W.C.,**
530 **Stepanyan, R.*, et al.* (2017). A molecular basis for water motion detection by the mechanosensory**
531 **lateral line of zebrafish. Nature communications *8*, 2234.**
532 **Coombs., S., Bleckmann., H., Fay., R.R., and Popper, A.N. (2014). The Lateral Line System (New**
533 **York: Springer).**
534 **Dijkgraaf, S. (1962). The functioning and significance of the lateral-line organs. Biological**
535 **Reviews of the Cambridge Philosophical Society *38: 51-105*.**
536 **Fan, Y., Wang, S., Hernandez, J., Yenigun, V.B., Hertlein, G., Fogarty, C.E., Lindblad, J.L., and**

537 **Bergmann, A. (2014). Genetic models of apoptosis-induced proliferation decipher activation of JNK**
538 **and identify a requirement of EGFR signaling for tissue regenerative responses in Drosophila. PLoS**
539 **genetics *10*, e1004131.**
540 **Flock, A., and Wersall, J. (1962). A study of the orientation of the sensory hairs of the receptor**
541 **cells in the lateral line organ of fish, with special reference to the function of the receptors. The**
542 **Journal of cell biology *15*, 19-27.**
543 **Kniss, J.S., Jiang, L., and Piotrowski, T. (2016). Insights into sensory hair cell regeneration from**
544 **the zebrafish lateral line. Current opinion in genetics & development *40*, 32-40.**
545 **Kurimoto, T., Yin, Y., Habboub, G., Gilbert, H.Y., Li, Y., Nakao, S., Hafezi-Moghadam, A., and**
546 **Benowitz, L.I. (2013). Neutrophils express oncomodulin and promote optic nerve regeneration. The**
547 **Journal of neuroscience : the official journal of the Society for Neuroscience *33*, 14816-14824.**
548 **Li, L., Yan, B., Shi, Y.Q., Zhang, W.Q., and Wen, Z.L. (2012). Live imaging reveals differing roles of**
549 **macrophages and neutrophils during zebrafish tail fin regeneration. The Journal of biological**
550 **chemistry *287*, 25353-25360.**
551 **Lopez-Schier, H., and Hudspeth, A.J. (2006). A two-step mechanism underlies the planar**
552 **polarization of regenerating sensory hair cells. Proceedings of the National Academy of Sciences of**
553 **the United States of America *103*, 18615-18620.**
554 **Lush, M.E., and Piotrowski, T. (2014). Sensory hair cell regeneration in the zebrafish lateral line.**
555 **Developmental dynamics : an official publication of the American Association of Anatomists *243*,**
556 **1187-1202.**
557 **Ma, E.Y., Rubel, E.W., and Raible, D.W. (2008). Notch signaling regulates the extent of hair cell**
558 **regeneration in the zebrafish lateral line. The Journal of neuroscience : the official journal of the**
559 **Society for Neuroscience *28*, 2261-2273.**
560 **Matsui., J.I., and Cotanchea., D.A. (2004). Sensory hair cell death and regeneration two halves**
561 **of the same equation. Hearing Science.**
562 **Mescher, A.L. (2017). Macrophages and fibroblasts during inflammation and tissue repair in**
563 **models of organ regeneration. Regeneration *4*, 39-53.**
564 **Mizutari, K., Fujioka, M., Hosoya, M., Bramhall, N., Okano, H.J., Okano, H., and Edge, A.S.**
565 **(2013). Notch inhibition induces cochlear hair cell regeneration and recovery of hearing after**
566 **acoustic trauma. Neuron *77*, 58-69.**
567 **Nechiporuk, A., and Raible, D.W. (2008). FGF-Dependent Mechanosensory Organ Patterning in**
568 **Zebrafish. Science *320*, 1774-1777.**
569 **Oesterle, E.C., and Stone, J.S. (2008). Hair Cell Regeneration: Mechanisms Guiding Cellular**
570 **Proliferation and Differentiation. In Hair Cell Regeneration, Repair and Protection, RJ Salvi , A.**
571 **Popper, and R. Fay, eds. (New York: Springer), pp. 141-197.**
572 **Olszewski, J., Haehnel, M., Taguchi, M., and Liao, J.C. (2012). Zebrafish Larvae Exhibit Rheotaxis**
573 **and Can Escape a Continuous Suction Source Using Their Lateral Line. PloS one *7*, e36661.**
574 **Pereira, T.C., Campos, M.M., and Bogo, M.R. (2016). Copper toxicology, oxidative stress and**
575 **inflammation using zebrafish as experimental model. Journal of applied toxicology : JAT *36*, 876-885.**
576 **Perez-Garijo, A., Shlevkov, E., and Morata, G. (2009). The role of Dpp and Wg in compensatory**
577 **proliferation and in the formation of hyperplastic overgrowths caused by apoptotic cells in the**
578 **Drosophila wing disc. Development *136*, 1169-1177.**

579 Popper, A.N., and Hoxter, B. (1984). Growth of a fish ear: 1. Quantitative analysis of hair cell
580 and ganglion cell proliferation. Hearing research *15*, 133-142.
581 Raphael, Y. (1992). Evidence for supporting cell mitosis in response to acoustic trauma in the
582 avian inner ear. J Neurocytol *21*, 663-671.
583 Renshaw, S.A., and Trede, N.S. (2012). A model 450 million years in the making: zebrafish and
584 vertebrate immunity. Disease models & mechanisms *5*, 38-47.
585 Roberson, D.W., Alosi, J.A., and Cotanche, D.A. (2004). Direct transdifferentiation gives rise to
586 the earliest new hair cells in regenerating avian auditory epithelium. Journal of Neuroscience
587 Research *78*, 461-471.
588 Romero-Carvajal, A., Navajas Acedo, J., Jiang, L., Kozlovskaja-Gumbriene, A., Alexander, R., Li,
589 H., and Piotrowski, T. (2015). Regeneration of Sensory Hair Cells Requires Localized Interactions
590 between the Notch and Wnt Pathways. Developmental cell *34*, 267-282.
591 Rubbini, D., Robert-Moreno, A., Hoijman, E., and Alsina, B. (2015). Retinoic Acid Signaling
592 Mediates Hair Cell Regeneration by Repressing p27kip and sox2 in Supporting Cells. The Journal of
593 neuroscience : the official journal of the Society for Neuroscience *35*, 15752-15766.
594 Ryoo, H.D., Gorenc, T., and Steller, H. (2004). Apoptotic cells can induce compensatory cell
595 proliferation through the JNK and the Wingless signaling pathways. Developmental cell *7*, 491-501.
596 Shimizu, N., Kawakami, K., and Ishitani, T. (2012). Visualization and exploration of Tcf/Lef
597 function using a highly responsive Wnt/β-catenin signaling-reporter transgenic zebrafish.
598 Developmental Biology *370*, 71-85.
599 Stone., J.S., and Rubel., E.W. (2000). Cellular studies of auditory hair cell regeneration in birds.
600 PNAS.
601 Suli, A., Watson, G.M., Rubel, E.W., and Raible, D.W. (2012). Rheotaxis in Larval Zebrafish Is
602 Mediated by Lateral Line Mechanosensory Hair Cells. PloS one *7*, e29727.
603 Thomas, E.D., Cruz, I.A., Hailey, D.W., and Raible, D.W. (2015). There and back again:
604 development and regeneration of the zebrafish lateral line system. Wiley Interdiscip Rev Dev Biol *4*,
605 1-16.
606 Tian, L., Hires, S.A., and Looger, L.L. (2012). Imaging neuronal activity with genetically encoded
607 calcium indicators. Cold Spring Harbor protocols *2012*, 647-656.
608 Yang, Y.X., Zheng, L.T., Shi, J.J., Gao, B., Chen, Y.K., Yang, H.C., Chen, H.L., Li, Y.C., and Zhen, X.C.
609 (2014). Synthesis of 5alpha-cholestan-6-one derivatives and their inhibitory activities of NO
610 production in activated microglia: discovery of a novel neuroinflammation inhibitor. Bioorganic &
611 medicinal chemistry letters *24*, 1222-1227.
612 Yorgason., J.G., Fayad., J.N., and Kalinec., F. (2006). Understanding drug ototoxicity: molecular
613 insights for preventionand clinical management. Biological Reviews.
614 Zhang, Q., Li, S., Wong, H.C., He, X.J., Beirl, A., Petralia, R.S., Wang, Y.X., and Kindt, K.S. (2018).
615 Synaptically silent sensory hair cells in zebrafish are recruited after damage. Nature
616 communications *9*, 1388.
617 Zhang, Q.X., He, X.J., Wong, H.C., and Kindt, K.S. (2016). Functional calcium imaging in zebrafish
618 lateral-line hair cells. Methods in cell biology *133*, 229-252.
619

620

621

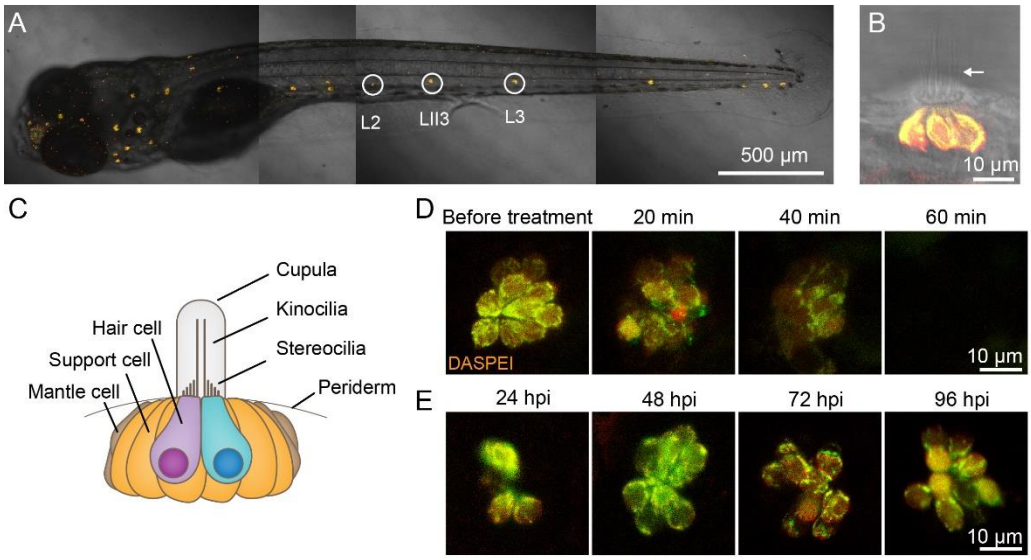


**Fig. 1 $CuSO_4$ damaged hair cells in lateral line of zebrafish.**

**(A)** Lateral line hair cells in a 6 day post fertilization (dpf) AB/WT zebrafish larvae are labeled with 0.05% DASPEI. L2, LII3 and L3 neuromasts are marked with circles. Scale bar represents 500 μm.

**(B)** Lateral view of a neuromast shows sensory hair cells in the center labeled with DASPEI and a bundle of kinocilia (arrow) extend out of the periderm. Scale bar represents 50 μm.

**(C)** A cartoon illustrating the structure of the neuromast.

**(D)**Time lapse imaging shows that when merged in 5 μM $CuSO_4$ solution, hair cells were gradually injured and damaged within 60 min. Scale bar represents 10 μm.

**(E)** DASPEI staining displays that hair cells regenerate completely within 96 hours post injured (hpi). Scale bar represents 10 μm.

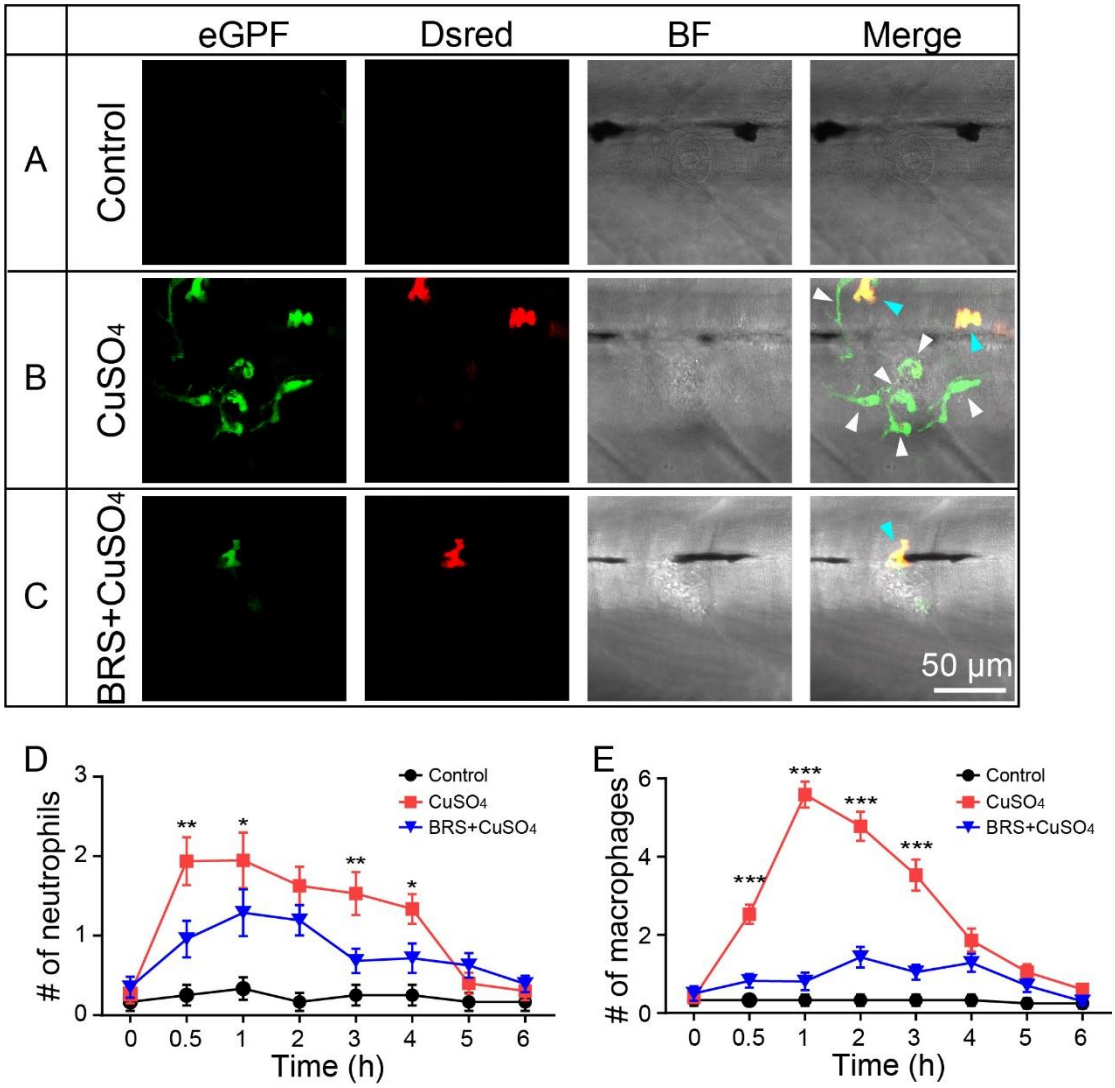


**Fig. 2 BRS-28 reduces the number of neutrophils and macrophages migrating to the injured neuromasts.**

**(A-C)** Live imaging (×40) displays the regions of L3 neuromasts of larvae at GFP channel, Dsred channel, and bright field (BF) channel and superimposed image in different group. Neutrophils (show both green and yollow fluorescence, indicated by white arrows) and macrophages (show olny green fluorescence, indicated by blue arrows) around the neuromasts can be observed in Tg(corola-eGFP; lyz-Dsred) larvae. They are almost absent from the neuromasts in Control group **(A)**. Many neutrophils and macrophages migrate to injured neuromasts in $CuSO_4$ group **(B)** while fewer neutrophils and macrophages migrate to injured neuromasts in BRS+$CuSO_4$ group **(C)**. The image is captured after adding $CuSO_4$ solution for 1 h. Scale bar represents 50

650 μm.

651 **(D-E)** Line charts reveal decreased numbers of neutrophils **(D)** and
652 macrophages **(E)** within a radius of 50 μm from the center of neuromasts at
653 different time points after adding $CuSO_4$ in BRS+$CuSO_4$ group (n≥16) than
654 $CuSO_4$ group (n≥15). Control group (n≥11) is observed at the same time
655 points.

656 To **(D)** and **(E)**, comparisons were performed by using two-way ANOVA,
657 with Tukey's multiple comparisons test. All Error bars show mean ± S.E.M., ***
658 P < 0.001, **P < 0.01,*P < 0.05.

659

660

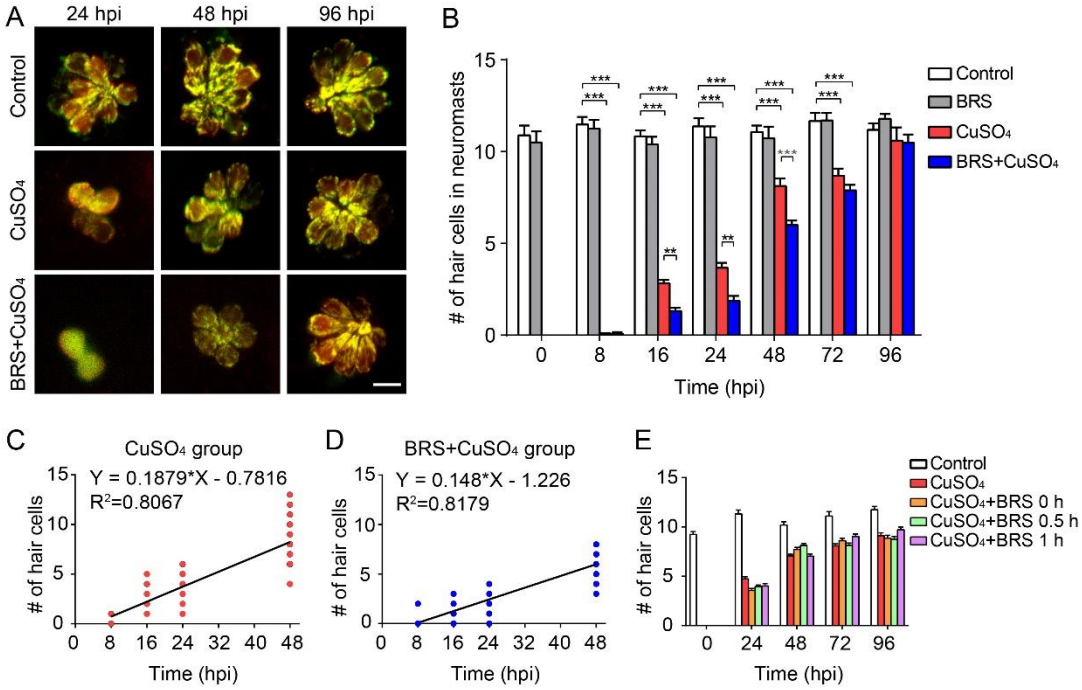


**Fig. 3 Suppressing inflammation delays hair cell regeneration.**

**(A)** Real-time imaging (×40) displays regenerated hair cells in the $CuSO_4$ and BRS+$CuSO_4$ group at 24, 48 and 96 hpi. Control group is taken at the same time point. Scale bar represents 10 μm.

**(B)** The numbers of regenerated hair cells were significantly decreased in BRS+$CuSO_4$ group than that in $CuSO_4$ group at 16 (P=0.0061), 24 (P=0.0021) and 48(P<0.0001) hpi. At 96 hpi, hair cells in both $CuSO_4$ group and BRS+$CuSO_4$ group regenerated to normal levels.

Linear analysis in $CuSO_4$ group **(C)** and BRS+$CuSO_4$ group **(D)** were conducted on the number of regeneration within 48 hours. The slope in $CuSO_4$ group (0.1879) is higher than that in BRS+$CuSO_4$ group (0.148) and x-intercept in $CuSO_4$ group (4.16) is higher than that in BRS+CuSO4 group (8.287).

**(E)** When delay the time window of inflammatory suppression, there is no delay in the regeneration of hair cells. BRS-28 was added at the same time as $CuSO_4$ ($CuSO_4$+BRS 0 h group), or 30 minutes after the addition of $CuSO_4$

678 ($CuSO_4$+BRS 0.5 h group), or 1 hour after the addition of $CuSO_4$ ($CuSO_4$+BRS
679 1 h group)(n≥27 neuromasts in each time point of each group).
680 To **(B)** and **(E)**, comparisons were performed by using two-way ANOVA,
681 with Tukey's multiple comparisons test. All Error bars show mean ± S.E.M., ***
682 P < 0.001, **P < 0.01,*P < 0.05.
683

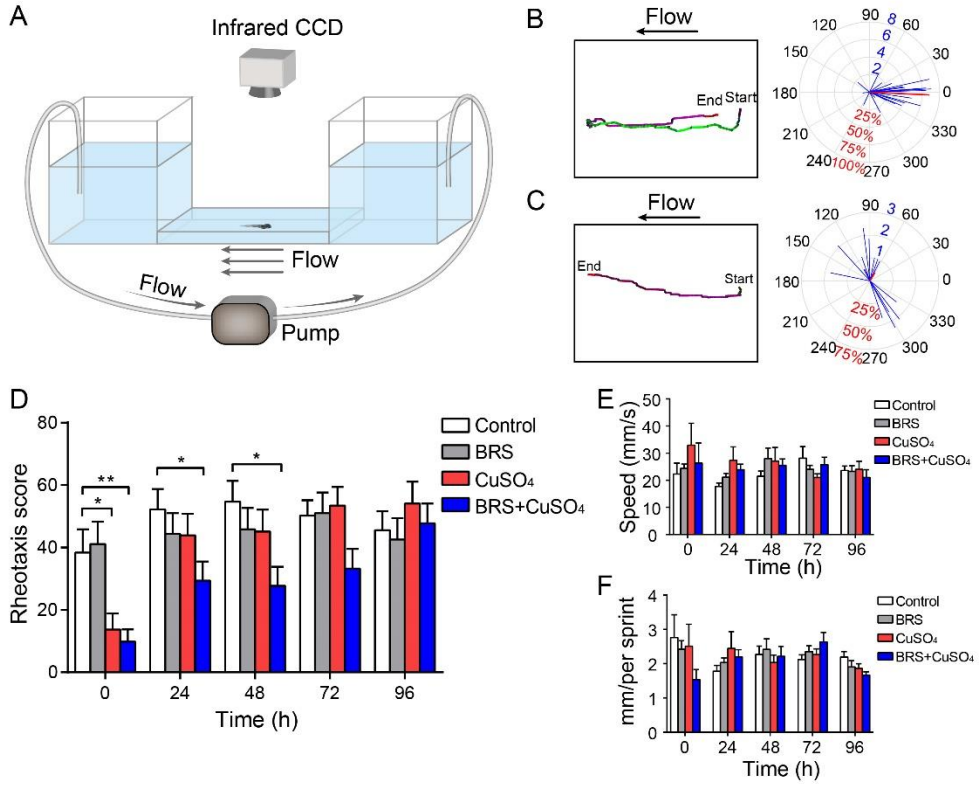


**Fig.4 The recovery of the functional of lateral line system was delayed when inflammation was suppressed.**

(**A**) A U-shaped tank was designed to test the rheotaxis behavior of larvae. A peristaltic pump was used to form flow at the bottom of the tank. Larvae were placed from the right platform, and they sense the water flow from right to left. Rheotaxis perform was recorded by an infrared CCD.

A larva with excellent rheotaxis **(B)** and a larva with poor rheotaxis **(C)** were analyzed by behavioral analysis software. Moving traces were plotted in left panels and the motion vector were displayed in right panels. The lengths of the blue segments represented the distance of each movement, and the direction of the blue segment represented the direction of that movement. The length of the red line segment was the ratio of motion vectors sum to the motion arithmetic sum and the direction was the direction of the sum of the vectors.

**(D)** Rheotaxis score revealed that at 24 and 48 hpi, the rheotaxis of

BRS+$CuSO_4$ group was significantly lower than that of Control group. On the contrary, the rheotaxis of $CuSO_4$ group was not significantly different from that of Control group within 24 hpi.

The speed **(E)** and distance **(F)** of larvae swimming at each time were consistent within different times and between different groups.

To **(D-F)**, comparisons were performed by using two-way ANOVA, with Tukey's multiple comparisons test. All Error bars show mean ± S.E.M., **P < 0.01,*P < 0.05.

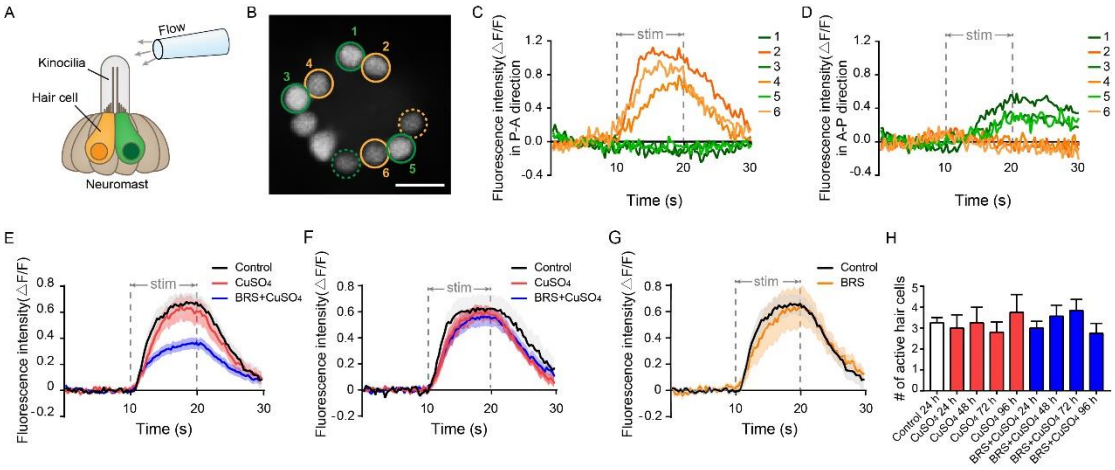


**Fig.5 Calcium imaging revealed the function of a single neuromast after hair cell regeneration**

**(A)** Schematic diagram shows an electrode filled with fluid is located about 100 μm away from the top of kinocilia to stimulate the neuromast. The yellow and green hair cells represent different polarities.

**(B)** When stimulated by the flow, only a part of hair cells respond in this focal plane (circled cells), and some are far from this focal plane (dashed circled cells). The No. 2, 4, and 6 active hair cells (yellow circles) only respond to the flow in P-A direction **(C)**. At the same time, the No. 1, 3, and 5 active hair cells (green circles) only respond to the flow in A-P direction **(D).** Scale bar in **(B)** represents 10 μm.

**(E)** The fluorescence intensity (ΔF/F) of the BRS + $CuSO_4$ group is significantly lower than that of the $CuSO_4$ group in the Early Stage of regeneration (within 48 hpi)( $P < 0.001$).

**(F)** The ΔF/F of BRS+$CuSO_4$ group is not significantly different from that of Control group and $CuSO_4$ group in the Late Stage of regeneration (72-96 hpi)

**(G)** There is no difference in ΔF/F between the BRS group and the Control group.

**(H)** During the regeneration process, the number of active hair cells in $CuSO_4$ and BRS+$CuSO_4$ group is basically the same, and did not increase

732 with the total number of regenerated hair cells.

733 To **(E-H)**, comparisons were performed by using one-way ANOVA, with
734 Tukey's multiple comparisons test.

735

736

737

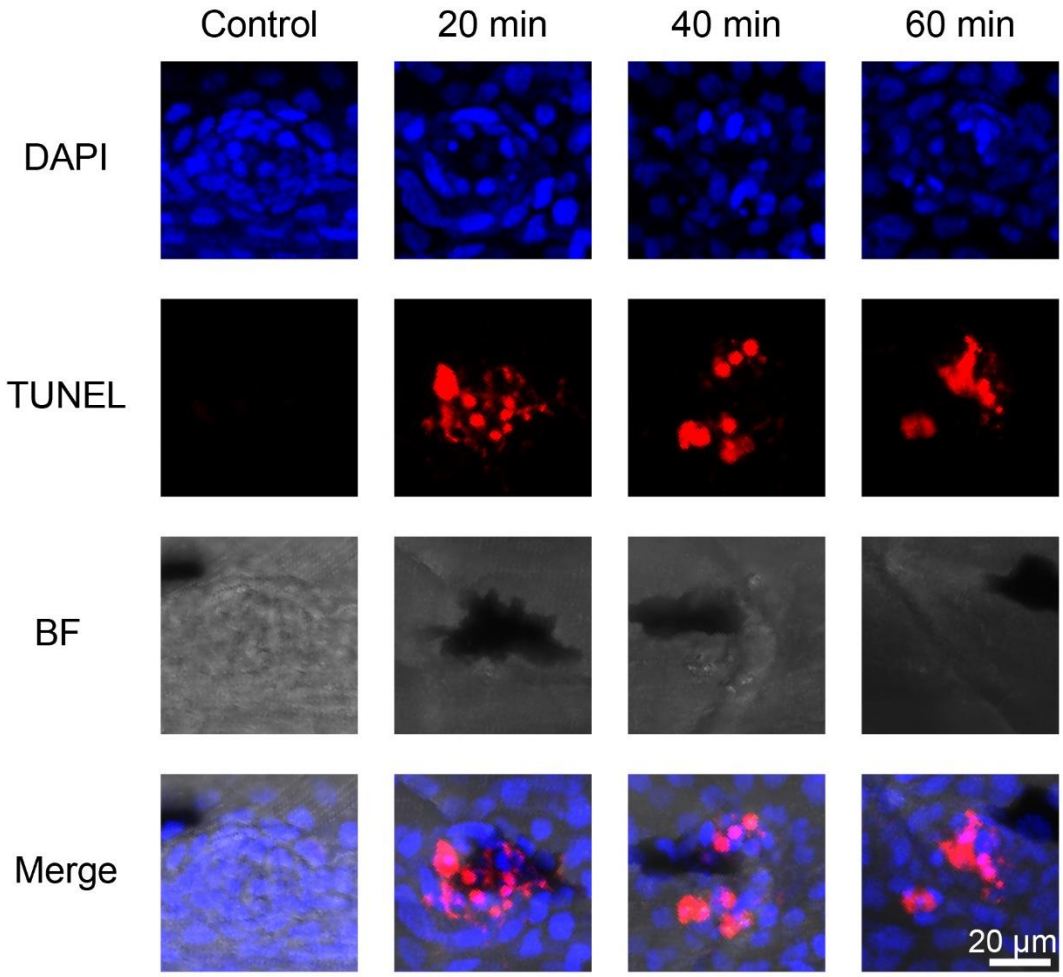


**Supplementary Fig. 1 $CuSO_4$ caused apoptosis in hair cells.**

TUNEL assay revealed hair cells occurred apoptosis when treated with $CuSO_4$. Nuclei were stained with DAPI. BF: Bright Field. Scale bar represents 20 μm.

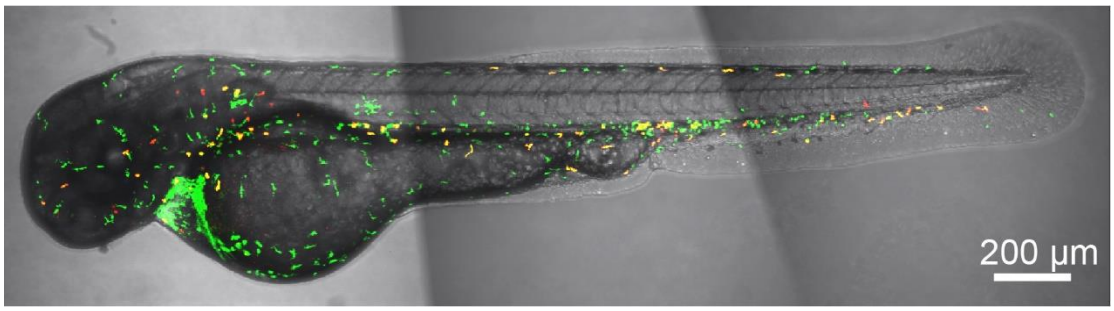


**Supplementary Fig. 2 Tg(corola-eGFP; lyz-Dsred) transgenic line could mark both neutrophils and macrophages.**

In Tg(corola-eGFP; lyz-Dsred) transgenic line, neutrophils co-expressed *lyz-Dsred* and *coro1a-GFP* and show yellow fluorescence after these two channels are merged, while macrophages only express *coro1a-GFP* and show green fluorescence. Scale bar represents 200 μm.

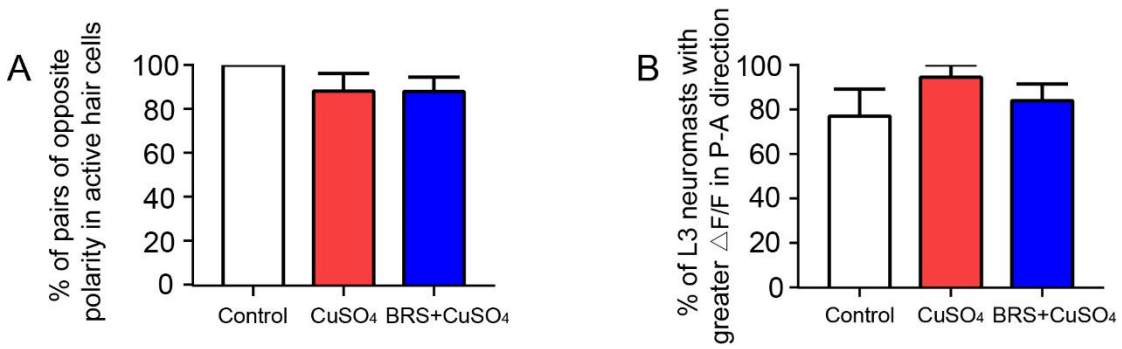


**Supplementary Fig. 3 Most active hair cells are polar in pairs and are sensitive to flow in the P-A direction.**

**(A)** Most hair cells that responded to the flow in the opposite direction come in pairs.

**(B)** The fluorescence intensity of hair cells responding to P-A direction is significantly higher than that of hair cells responding to A-P direction.

To **(A,B)**, comparisons were performed by using one-way ANOVA, with Tukey's multiple comparisons test. All Error bars show mean ± S.E.M.